Bull. Korean Chem. Soc. **2014**, Vol. 35, No. 6 1837
http://dx.doi.org/10.5012/bkcs.2014.35.6.1837

Notes

Solvothermal Synthesis of Supercrystals of Hematite *via* the Self-assembly of Nanocubes

Young-Sik Cho, Seung-Hyun Lee, Myeong-Jin Kim, and Young-Duk Huh*

*Department of Chemistry, Dankook University, Gyeonggi-Do 448-701, Korea. *E-mail: ydhuh@dankook.ac.kr*
Received December 30, 2013, Accepted February 5, 2014

Key Words : Hematite, Self-assembly, Supercrystal, Nanocube

In recent years, self-assembled superlattices of inorganic oxides have been prepared with many different types of packing to assess their applications in electronics, optics, and magnetism.[1-6] The simplest superlattice consists of nanocrystals with all the same size and shape. Face-centered cubic (fcc) and hexagonal close-packed (hcp) structures with the maximum packing density of 74% are usually formed from spherical nanocrystals.[7] For cubic nanocrystals, the face-to-face cubic structure can be formed with the maximum packing density of 100%.[8] Most superlattices are fabricated by placing a drop of a nanocrystal colloid onto a transmission electron microscopy (TEM) copper grid or silicon plate and facilitating the subsequent evaporation of the solvent. These techniques usually provide two- and three-dimensional superlattices with sizes of a few hundred nanometers.[9] However, the size of superlattices and degree of self-assembly depend strongly on the delicate evaporation conditions. Therefore, it is hard to produce the regular sizes of superlattcies in a large-scale production. In addition, three-dimensional micron-sized macroscopic supercrystals cannot be prepared with these techniques. Moreover, the large-scale production for the applications in electronics and magnetism cannot be produced in these solvent evaporation techniques. Therefore, we need to develop a simple synthetic method for the large-scale preparation of three-dimensional supercrystals of inorganic oxides that does not require a solvent evaporation process.

There are many different types of iron oxides, such as hematite (α-Fe_2O_3), maghemite (γ-Fe_2O_3), and magnetite (Fe_3O_4). α-Fe_2O_3 is the most stable iron oxide under ambient conditions; it is an n-type semiconductor with a band gap of 2.1 eV, and is used in catalysis, gas sensors, and lithium-ion batteries.[10-12] α-Fe_2O_3 crystals with various morphologies, such as nanocubes, nanorods, nanotubes, nanodiscs, dodecahedra, and octadecahedra, have been prepared. Nanocubes of α-Fe_2O_3 with 20 nm sides were obtained by using $FeCl_3 \cdot 6H_2O$, oleic acid, and NaOH in ethanolic solution.[13] α-Fe_2O_3 nanocubes with 15 nm sides have also been synthesized through the decomposition of an iron-oleate complex under hydrothermal conditions.[14] α-Fe_2O_3 nanorods were prepared by using the sol-gel mediated synthetic method.[15] α-Fe_2O_3 nanodiscs were synthesized by using 1,10-phenanthroline as a complexing agent in the presence of NaOH under hydrothermal conditions.[16] Dodecahedral and octadecahedral α-Fe_2O_3 crystals were synthesized with a hydrothermal reaction assisted by fluoride anions.[17] Most successful preparations of two-dimensional superlattices of α-Fe_2O_3 have used solvent evaporation methods on the TEM grids for the examination of the self-assembly with very small-scale production. However, the large-scale fabrication of macroscopic supercrystals of α-Fe_2O_3 has not been reported. Here we present a simple method for producing micron-sized supercrystals of α-Fe_2O_3, in which a solvothermal reaction is performed in a toluene solution containing Fe-oleate and tetraoctylammonium hexacyanoferrate (II) ((TOA)-[$Fe(CN)_6$]) complexes. To the best of authors' knowledge, this is the first report for the large-scale production of micron-sized supercrystals of α-Fe_2O_3. The mechanism of the formation of three-dimensional supercrystals of α-Fe_2O_3 *via* the self-assembly of nanocubes is also discussed.

Figure 1 shows SEM images at low and high magnifications of the micron-sized α-Fe_2O_3 supercrystals prepared with the solvothermal reaction. The product is composed of cubic crystals with an average side length of 2.6 μm. The regular size of supercrystals is obtained, as shown in Figure 1(a). Since the regular size of supercrystals cannot be produced by the solvent evaporation method, this solvothermal reaction is novel method for the preparation of micron-sized supercrystals in a large-scale production. Figure 1(b) shows a high magnification SEM image of an individual cubic

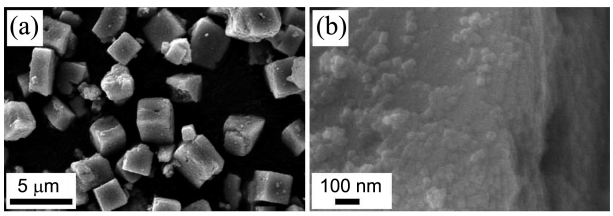

Figure 1. (a) Low magnification and (b) high magnification SEM images of the α-Fe_2O_3 products obtained from the solvothermal reaction.

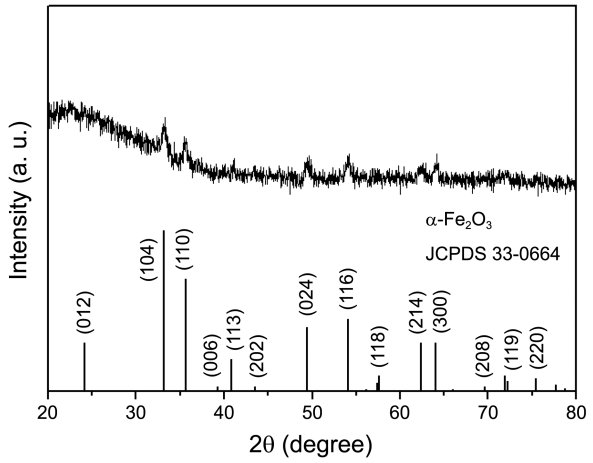

Figure 2. Powder XRD pattern of the α-Fe_2O_3 products obtained from the solvothermal reaction.

crystal. Assemblies of small nanocubes are evident on the surfaces of the supercrystal, which indicates that the micron-sized cubic supercrystals are formed by the self-assembly of the nanocubes.

There are many iron oxides, such as α-Fe_2O_3, γ-Fe_2O_3, and Fe_3O_4. Figure 2 shows the typical X-ray diffraction (XRD) patterns of the product obtained from the solvothermal reaction. Even though there are weak signal intensities with large backgrounds, all of the diffraction peaks match with literature data of α-Fe_2O_3 (JCPDS 33-0664, $a = 0.5035$ nm, $c = 1.3748$ nm). This indicates that α-Fe_2O_3 product has been prepared. In general, it is well known that the large XRD backgrounds are observed due to the X-ray induced fluorescence of α-Fe_2O_3. Therefore, Raman spectrum is used to examine the α-Fe_2O_3 products. Raman spectra for wave numbers below 1000 cm^{-1} can provide clear assignments of iron oxides.[18] Figure 3(a) shows the Raman spectrum of the as-prepared cubic supercrystal. The inset shows an optical image of the cubic supercrystal used in the recording of the Raman spectrum. The peaks at 284, 397, 484, and 597 cm^{-1} correspond to the E_g, E_g, A_{1g}, and E_g modes of α-Fe_2O_3, respectively.[19] The two-magneton scattering peak of α-Fe_2O_3 is also evident at 1276 cm^{-1}. All of the Raman peaks match the reported data for α-Fe_2O_3. The Raman peaks of γ-Fe_2O_3 at 365, 511, and 700 cm^{-1} and those of Fe_3O_4 at 310, 554, and 672 cm^{-1} were not observed.[19] These results indicate that α-Fe_2O_3 products have successfully been prepared. Fourier transform infrared (FT-IR) spectra provide information about capped organic molecules on surface nanomaterials. Figure 3(b) shows the FT-IR spectra of sodium oleate and of the cubic supercrystals of α-Fe_2O_3. In the FT-IR spectrum of the supercrystals of α-Fe_2O_3, the bands at 2924 and 2853 cm^{-1} correspond to the asymmetric and symmetric stretching modes respectively of the methylene (-CH_2-) groups. The characteristic band at 1410 cm^{-1} is assigned to symmetric COO^- stretches. A large shift in the symmetric COO^- stretch

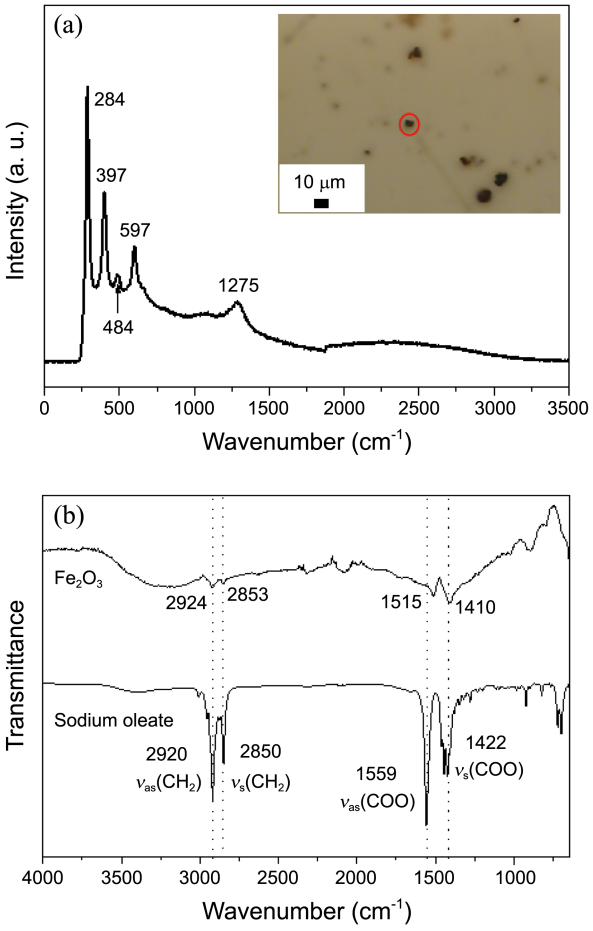

Figure 3. (a) Raman and (b) FT-IR spectra of the α-Fe_2O_3 products obtained from the solvothermal reaction. The inset in (a) shows a microscopy image of the sample used in the recording of the Raman spectrum.

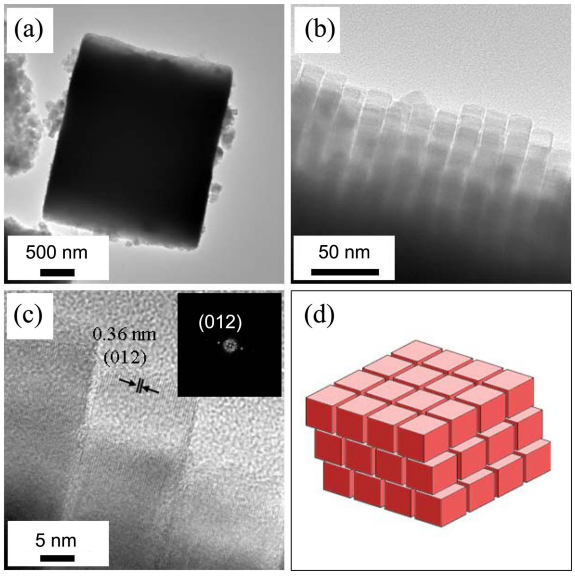

Figure 4. (a) HRTEM image of an individual supercrystal of α-Fe_2O_3. (b, c) High magnification HRTEM images of the self-assembled superlattice on the edge of the supercrystal. The inset in (c) shows the FFT pattern of an individual nanocube. (d) A schematic structural diagram of a cubic supercrystal formed by self-assembled nanocubes in the face-to-face configuration and shifted by only one axis in the horizontal plane.

band at 1515 cm^{-1} is observed. Therefore, XRD pattern, Raman spectrum, and FT-IR spectrum indicate that oleate ions are coated onto the surfaces of the nanocubes of α-Fe_2O_3. The oleate ions induce the self-assembly of nanocubes to form micron-sized cubic supercrystals.

The morphology of the synthesized supercrystals of α-Fe_2O_3 was characterized by using high-resolution transmission microscopy (HRTEM), and a schematic diagram of this morphology is shown in Figure 4(d). Figure 4(a) shows a single supercrystal with a length of 2.3 μm and a height of 2.9 μm. A series of self-assembled superlattices of nanocubes on the edge of the supercrystal were obtained, as shown in Figure 4(b). The nanocubes have a mean length of 15 nm, which includes the space between the nanocubes, and are self-assembled into a three-dimensional cubic structure. Some two-dimensional square arrays can also be seen at the edge of the supercrystal, as shown in Figure 4(c). From the value measured for the length of the sides of the nanocubes, we can calculate the number of self-assembled nanocubes from the width and height of the supercrystal. The estimated total number of nanocubes in the supercrystal is approximately 5,000,000 (150 × 190 × 175). Since the mean length of the nanocubes is approximately 15 nm, and the average center to center distance between adjacent nanocubes is approximately 17 nm, the average inter-nanocube gap in the superlattice is approximately 2 nm, which is greater than the layer distance of sodium oleate, 1.7 nm.[20] Therefore, the sodium oleate molecules could be arranged in a tilted bilayer structure between adjacent nanocubes. The van der Waals interactions of the long-chain alkyl groups of the oleate ions induce the self-assembly of the nanocubes to form a stable cubic supercrystal. The inset in Figure 4(c) shows the fast Fourier transform (FFT) pattern of an individual nanocube in a supercrystal with a lattice spacing of 0.36 nm, which corresponds to the (012) plane of rhombohedral α-Fe_2O_3 (JCPDS 33-0664, a = 0.5035 nm, c = 1.3748 nm), and shows that the nanocubes are high-quality single-crystalline.

Interestingly, in the TEM images in Figures 4(b) and 4(c) we can clearly see the one directional spacing line on the horizontal plane of the self-assembled cubic arrangement of the supercrystal. When a perfect face-to-face cubic supercrystal is formed, the grid patterns of the spacing lines on the horizontal plane should be visible. This result indicates that the nanocubes are well arranged and shifted one axis in the horizontal plane from the perfect face-to-face configuration. Since more than 150 nanocubes are arranged in each direction, and 5,000,000 nanocubes are closely packed in three dimensions, the formation of a perfect three-dimensional face-to-face configuration is almost impossible. Moreover, the structure with one axis shifted in the horizontal plane has a packing density of 100%, as is the case for the perfect face-to-face configuration. Thus the SEM and TEM images show that the nanocubes have a tendency to assemble into three-dimensional arrays in a regular simple cubic face-to-face pattern with one axis shifted along the horizontal plane. Figure 4(d) shows a schematic structural diagram of a cubic supercrystal consisting of nanocubes self-assembled in this configuration.

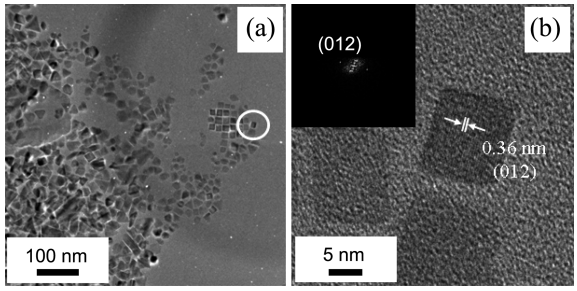

Figure 5. (a) Low magnification and (b) high magnification TEM images of α-Fe_2O_3 products prepared *via* solvothermal reactions in the absence of TOA-[$Fe(CN)_6$] complex. The inset in (b) shows the FFT pattern of an individual nanocube.

To investigate the critical factors in the formation of these supercrystals, we also prepared α-Fe_2O_3 products *via* the solvothermal reaction from the iron-oleate complex in the absence of the TOA-[$Fe(CN)_6$] complex, with all other conditions kept constant. Various shapes such as nanocubes and nanotriangles were obtained, as shown in Figure 5(a). Some self-assembled nanocubes with a mean side length of 14 nm were obtained, as shown in Figure 5(b). However, strong self-assembly behavior such as the formation of a supercrystal did not occur, which indicates that the presence of TOA-[$Fe(CN)_6$] plays an important role in the formation of the supercrystals.

Prussian blue, $Fe_4[Fe(CN)_6]_3 \cdot xH_2O$, has a face-centered cubic structure with the Fe^{3+} ions coordinating the nitrogen atoms and the Fe^{2+} ions to the carbon, which can give rise to three-dimensional Fe^{3+}-NC-Fe^{2+}-CN-Fe^{3+} coordination polymer structures.[21] Micron-sized Prussian blue crystals are easily obtained by reacting Fe^{3+} ions and $[Fe(CN)_6]^{4-}$ ions at room temperature because of their strong chemical stability. By calcinating Prussian blues in the temperature range 250 °C to 400 °C, α-Fe_2O_3 and γ-Fe_2O_3 have been prepared.[22] Therefore, Prussian blue is considered a precursor for the preparation of iron oxides.[23] Since only α-Fe_2O_3 products were prepared in this study, $[Fe(CN)_6]^{4-}$ ions were not used as reactants for α-Fe_2O_3 products. When the stable cubic Prussian blue precursor is used in the solvothermal reaction below 200 °C, a small number of Fe^{3+} ions are released from the $Fe_4[Fe(CN)_6]_3$ precursor. The Fe^{3+} ions react with oxygen in air to form α-Fe_2O_3. The cubic structure of Prussian blue could be used as a template. Once the Fe^{3+} ions have reacted with oxygen to form nanocubic α-Fe_2O_3, the adjacent $Fe(CN)_6^{4-}$ ions are dissolved in the solution. Nanocubes of α-Fe_2O_3 do form and are confined within the framework of the Prussian blue lattice, and the nanocubes assemble with adjacent nanocubes and finally form a micron-sized supercrystal. The detailed mechanism of the formation of supercrystals of α-Fe_2O_3 is under investigation. This study is the first report of the formation of micron-sized supercrystals consisting of close-packed nanocubes of α-Fe_2O_3 without the use of any solvent evaporation processes.

In conclusion, we have presented a simple synthetic method for the preparation of supercrystals of α-Fe_2O_3 from Fe-

oleate and TOA-[$Fe(CN)_6$] complexes *via* a solvothermal reaction. Micron-sized cubic supercrystals were obtained as precipitated products without the use of any solvent evaporation processes. The supercrystals of α-Fe_2O_3 are composed of approximately 5,000,000 nanocubes with a mean side length of 15 nm. The self-assembly of nanocubes of α-Fe_2O_3 result in a face-to-face configuration with only one axis shifted in the horizontal plane.

Experimental Section

$FeCl_3 \cdot 6H_2O$ (Aldrich), $K_4Fe(CN)_6$ (Aldrich), sodium oleate (TCI), oleic acid (Aldrich), and tetraoctylammonium bromide (TOABr, Aldrich) were used as received. In a typical synthesis of α-Fe_2O_3 supercrystals, 0.10 M $FeCl_3 \cdot 6H_2O$ was dissolved in 20 mL water. 1.83 g sodium oleate, 5.0 mL oleic acid, and 40 mL toluene were then added to the solution. The water-toluene bilayer mixture was vigorously stirring for 1 h at room temperature to allow the transfer of Fe^{3+} ions from the aqueous solution to the toluene phase through coordination with the oleate anions to form iron-oleate complexes. 3.28 g TOABr in 40 mL toluene was then added to 20 mL aqueous solution of $Fe(CN)_6^{4-}$ ions to obtain the TOA-[$Fe(CN)_6$] complexes into the toluene phase. The two toluene solutions containing the Fe-OA and TOA-[$Fe(CN)_6$] complexes were mixed under stirring. After mixing the two optically transparent solutions, the resulting solution was transferred to a 100 mL Teflon-lined autoclave. To prepare the α-Fe_2O_3 supercrystals, solvothermal reactions were conducted at 180 ^oC for 72 h. The product was collected by centrifuging the solution at 4000 rpm for 10 min. The precipitated products were washed several times with water and ethanol, and dried at 60 ^oC for 12 h.

The α-Fe_2O_3 product was examined with a Raman microscope (Kaiser, RamanRxn Microprobe). The capping organic compound in the supercrystals of α-Fe_2O_3 was examined by using an FT-IR spectrometer (Perkin Elmer 100 FT-IR). The α-Fe_2O_3 product was also analyzed by powder X-ray diffraction (XRD, PANanlytical, X'pert-pro MPD) using Cu K_α radiation. The morphologies of the supercrystals and the superlattice patterns of the nanocubes of α-Fe_2O_3 were examined by using scanning electron microscopy (SEM, Hitachi S-4300) and high resolution transmission electron microscopy (HRTEM, JEOL JEM-3010), respectively.

References

1. Talapin, D. V. *ACS Nano* **2008**, *2*, 1097.
2. Park, J.; An, K.; Hwang, Y.; Park, J. G.; Noh, H. J.; Kim, J. Y.; Park, J. H.; Hwang, N. M.; Hyeon, T. *Nature Mater.* **2004**, *3*, 891.
3. Ahniyaz, A.; Sakamoto, Y.; Bergström, L. *Proc. Natl. Acad. Sci.* **2007**, *104*, 17570.
4. Quan, Z.; Fang, J. *Nano Today* **2010**, *5*, 390.
5. Nguyen, T. D.; Do, T. O. *J. Phys. Chem. C* **2009**, *113*, 11204.
6. Kinge, S.; Crego-Calama, M.; Reinhoudt, D. N. *ChemPhysChem* **2008**, *9*, 20.
7. Stoeva, S. I.; Prasad, B. L. V.; Uma, S.; Stoimenov, P. K.; Zaikovski, V.; Sorensen, C. M.; Klabunde, K. J. *J. Phys. Chem. B* **2003**, *107*, 7441.
8. Chan, H.; Demortière, A.; Vukovic, L.; Král, P.; Petit, C. *ACS Nano* **2012**, *6*, 4203.
9. Zhang, J.; Kumbhar, A.; He, J.; Das, N. C.; Yang, K.; Wang, J. Q.; Wang, H.; Stokes, K. L.; Fang, J. *J. Am. Chem. Soc.* **2008**, *130*, 15203.
10. Mou, X.; Wei, X.; Li, Y.; Shen, W. *CrystEngComm* **2012**, *14*, 5107.
11. Wang, G.; Gou, X.; Horvat, J.; Park, J. *J. Phys. Chem. C* **2008**, *112*, 15220.
12. Wang, Z.; Luan, D.; Madhavi, S.; Li, C. M.; Lou, X. W. *Chem. Commun.* **2011**, 8061.
13. Liang, X.; Wang, X.; Zhuang, J.; Chen, Y.; Wang, D.; Li, Y. *Adv. Funct. Mater.* **2006**, *16*, 1805.
14. Wang, S. B.; Min, Y. L.; Yu, S. H. *J. Phys. Chem. C* **2007**, *111*, 3551.
15. Woo, K.; Lee, H. J.; Ahn, J. P.; Park, Y. S. *Adv. Mater.* **2003**, *15*, 1761.
16. Mehdizadeh, R.; Saghatfororoush, L. A.; Sanati, S. *Superlattices Microstruct.* **2012**, *52*, 92.
17. Lv, B.; Liu, Z.; Tian, H.; Xu, Y.; Wu, D.; Sun, Y. *Adv. Funct. Mater.* **2010**, *20*, 3987.
18. Jubb, A. M.; Allen, H. C. *ACS Appl. Mater. Interfaces* **2010**, *2*, 2804.
19. Chamritski, I.; Burns, G. *J. Phys. Chem. B* **2005**, *109*, 4965.
20. Bai, F.; Wang, D.; Huo, Z.; Chen, W.; Liu, L.; Liang, X.; Chen, C.; Wang, X.; Peng, Q.; Li, Y. *Angew. Chem. Int. Ed.* **2007**, *46*, 6650.
21. Lee, S. H.; Huh, Y. D. *Bull. Korean Chem. Soc.* **2012**, *33*, 1078.
22. Hu, M.; Belik, A. A.; Imura, M.; Mibu, K.; Tsujimoto, Y.; Yamauchi, Y. *Chem. Mater.* **2012**, *24*, 2698.
23. Zboril, R.; Machala, L.; Mashlan, M.; Sharma, V. *Cryst. Growth Des.* **2004**, *4*, 1317.